Study of Mass-Transport Limited Corrosion Using Pine Rotating Cylinder Electrodes

An Overview of Theory and Practice

This technical note addresses two aspects of electrochemical testing using the Rotating Cylinder Electrode (RCE). First, the fundamental hydrodynamic behavior at a rotating cylinder is summarized, including equations which predict the mass transport limited corrosion current at an RCE. Second, a means of selecting the suitable rotation rate for an RCE test is discussed, with emphasis being placed on matching a particular rotation rate to a particular flow velocity in a smooth pipe. In addition, a bibliography of significant reports regarding the RCE is provided.

Introduction

Corrosion processes can accelerate significantly under extreme environmental conditions such as high temperature, high pressure, and turbulent fluid flow. When troubleshooting a field corrosion problem, a researcher often needs to return to the lab and reproduce the same (or similar) harsh conditions in a controlled setting. While familiar laboratory equipment for temperature control (ovens, water baths) and pressure control (autoclaves) is generally readily available and easy to use, recreating a fluid flow condition generally poses a larger challenge to the researcher. Laboratory flow loop systems often require complex (*i.e.*, expensive) plumbing, maintenance, and calibration to reliably and reproducibly move fluid past a metal sample. But the need for this type of large-scale laboratory equipment can often be avoided by moving the metal sample with respect to the fluid instead.

One convenient instrument[1–35] for rapidly moving a metal sample with respect to a fluid is the **Rotating Cylinder Electrode** (RCE). This apparatus includes an electrode rotator and a control unit (see Figure 1) capable of precisely adjusting the rotation rate of a vertically oriented shaft. A special tip capable of holding a cylindrical shaped metal sample is mounted at the lower end of the shaft. The tip is fashioned primarily from chemically inert and electrically insulating materials (such as Teflon or KEL-F), but buried within the tip is a metal shank which provides mechanical stability and also electrical contact with the metal cylinder sample (see Figure 2).

When immersed and rotated in a test solution, the hydrodynamic conditions generated by the RCE, even at low rotation rates, are generally quite turbulent[1–5]. This makes the RCE an ideal probe for studying corrosion processes[12–15] under low velocity, but turbulent conditions. By adjusting the RCE

Figure 1: Pine AFMSRCE Electrode Rotator (for use with Rotating Cylinder Electrodes)

Figure 2: Rotating Cylinder Electrode Tip (easily taken apart to replace metal sample)

rotation rate up or down (typically in the range from 200 to 2000 RPM), it is possible to tune the hydrodynamic conditions[20–35] adjacent to the metal sample. The ideal goal is to adjust the rotation rate so that the laboratory fluid flow conditions match (or mimic) those found in the field. Once this is accomplished, the corrosion process can be monitored by classic mass loss methods or by electrochemical methods such as Linear Polarization Resistance (LPR)[21–22] or Electrochemical Impedance Spectroscopy (EIS)[14,24].

Tuning Turbulent Flow

At very slow rotation rates, the solution near a rotating cylinder flows with a regular and smooth motion called *laminar flow*. As the rotation rate increases, the solution flow becomes more complex. While the layer of solution in direct contact with the cylinder continues to cling to the surface, the shear stress between this layer and layers further from the cylinder begins to spin off vortices. At this point, the solution flow transitions from laminar to *turbulent flow*, and as the rotation rate increases, the vortices themselves spawn further vortices.

The transition from laminar to turbulent flow is often characterized using the Reynolds Number (RE) to quantify the ratio between inertial forces and viscous forces in a solution. For a rotating cylinder electrode[1–3] with outer diameter, d_{cyl} (cm), and radius, $r_{cyl} = d_{cyl} / 2$, the Reynold's Number is

$$\mathrm{RE} = U_{cyl}\, d_{cyl}\, \rho \,/\, \mu \qquad (1)$$

where ρ is the solution density (g cm^{-3}), and μ is the absolute viscosity of the solution (g cm^{-1} s^{-1}). The linear velocity, U_{cyl} (cm s^{-1}), at the outer surface of the cylinder is given by

$$U_{cyl} = \omega\, r_{cyl} = \pi\, d_{cyl}\, F \,/\, 60 \qquad (2)$$

where the rate can either be expressed as the angular rotation rate, ω (rad s^{-1}), or as F (RPM).

In general, for a rotating cylinder, when the Reynolds Number is greater than 200, then the flow is turbulent.

For all but the very slowest rotation rates, the turbulent condition is the norm. So, for the typical Pine RCE shown in Figure 2 (which has a diameter of 1.2 cm), rotation rates between 5 and 2000 RPM correspond to a range of Reynolds Numbers spanning several orders of magnitude (see Table I). The transition from laminar to turbulent flow occurs just above 20 RPM, when the Reynolds Number exceeds 200. It is worth noting that this transition occurs at a relatively small rotation rate, making the RCE an ideal tool for studying turbulent flow at low velocity—precisely the condition frequently found in pipeline infrastructures. Higher turbulent velocities are also easily accessible at higher rotation rates.

Mass Transport

The turbulent flow at the RCE can bring material from the solution to the surface of the cylinder, and it can also carry material away from the surface. In the context of a corrosion study, the rate of mass transport to and from the metal surface is often the factor which governs the rate of corrosion. A familiar example would be a corrosion process which is limited by how fast oxygen can be transported from the solution to the metal surface.

Early reports by Eisenberg[1,2] provide the most

Table I – Hydrodynamic Computations for a Typical* Rotating Cylinder Electrode in Water

Rotation Rate F (RPM)	Rotation Rate ω (rad / sec)	Surface Velocity* U_{cyl} (cm / sec)	Wall Shear Stress* τ_{cyl} (g cm^{-1} s^{-2})	Reynolds Number* Re (unitless)
5	0.524	0.31	0.0025	42
10	1.047	0.62	0.0082	84
20	2.094	1.26	0.0267	169
50	5.236	3.14	0.1270	422
100	10.47	6.28	0.4125	844
200	20.94	12.6	1.3402	1688
500	52.36	31.4	6.3631	4219
1000	104.7	62.8	20.674	8438
2000	209.4	125.7	67.169	16876

* These quantities assume a typical Pine RCE tip with outer diameter 1.2 cm rotating in water at 25ºC. For pure water at 25ºC, the density is 0.997 g cm^{-3} and the absolute viscosity is 0.00891 g cm^{-1} s^{-1}.

commonly accepted description for RCE mass transport. In particular, the mass transfer coefficient, K_M (cm s^{-1}) to a rotating cylinder is given by the following relationship:

$$K_M = (D / d_{cyl})\,\mathrm{SH}$$
$$= (D / d_{cyl})\,(0.0791\ \mathrm{RE}^{0.7}\ \mathrm{SC}^{0.356}) \quad (3)$$

where the diffusivity, D (cm^2 s^{-1}), is usually taken as the diffusion coefficient for the molecule or ion undergoing mass transport, and where SH and RE are the dimensionless Sherwood and Reynolds Numbers, respectively. The Schmidt Number, $\mathrm{SC} = \mu / (\rho\ D)$, is also a dimensionless number.

Combining equations (1) through (3), the overall mass transfer coefficient to an RCE can be expressed in one of three forms,

$$K_M = 0.0791\ d_{cyl}^{-0.3}\ (\mu / \rho)^{-0.344}\ D^{+0.644}\ U_{cyl}^{+0.7} \quad (4a)$$
$$= 0.0487\ d_{cyl}^{+0.4}\ (\mu / \rho)^{-0.344}\ D^{+0.644}\ \omega^{+0.7} \quad (4b)$$
$$= 0.0051\ d_{cyl}^{+0.4}\ (\mu / \rho)^{-0.344}\ D^{+0.644}\ F^{+0.7} \quad (4c)$$

depending upon whether the rotation rate is expressed in terms of linear surface velocity (U_{cyl}), angular rotation rate (ω), or rotations per minute (F). Note that the form shown in equation (4a) is that which is most often found in the literature.

Wall Shear Stress

The turbulent flow at the RCE induces a wall shear stress on the surface of the cylinder. Again, Eisenberg's original reports[1,2] offer a well-accepted[35] equation for the wall stress, τ_{cyl} (g cm^{-1} s^{-2}):

$$\tau_{cyl} = 0.0791\ \rho\ \mathrm{Re}^{-0.3}\ U_{cyl}^{2} \quad (5)$$

The wall shear stress for a typical Pine RCE tip (d_{cyl} = 1.2 cm) over a range of rotation rates is listed in Table I.

Electrochemical Measurements

When a rotating cylinder is used as the working electrode in a traditional three-electrode cell configuration, the corrosion behavior can be monitored[34–35] by measuring the electric current at the cylinder. Electrical connection to the metal cylinder is accomplished by means of a brush contact on the rotating shaft. A potentiostat is employed to impose various potentials on the cylinder electrode while simultaneously measuring the current. The potential signal applied to the cylinder may be a very slow voltage sweep (*i.e.*, Linear Polarization Resistance, LPR[21–22]), or it may involve a high frequency sinusoidal signal (*i.e.*, Electrochemical Impedance Spectroscopy[14,24], EIS).

Two other electrodes are also required to make an electrochemical measurement, a reference electrode (such as a silver/silver-chloride electrode) and a counter electrode. The counter electrode is often an even larger diameter cylinder (or wire loop) placed in the solution so that it surrounds the rotating cylinder. This helps to assure uniform current density at the RCE during the test.

In general, the mass transport limited current density, j_{LIM} (A cm^{-2}), observed in an electrochemical experiment is related to the mass transfer coefficient by the following relationship,

$$j_{LIM} = i_{LIM} / A = z\,F\,C\,K_M \quad (6)$$

where F is Faraday's Constant (96484.6 C / mol), i_{LIM} (A) is the limiting current, and A (cm^2) is the area of the electrode. To make full quantitative use of this

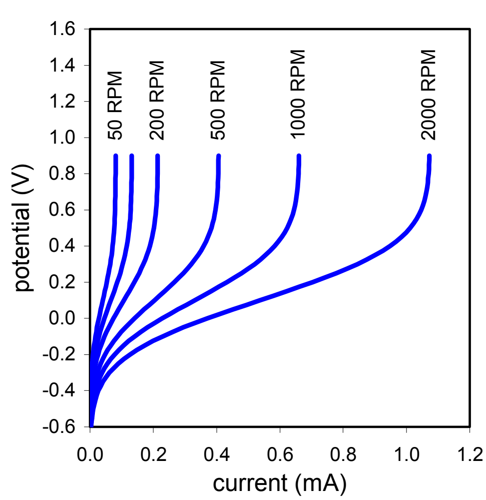

Figure 3: Example of a Series of LPR Scans Recorded at Various Rotation Rates

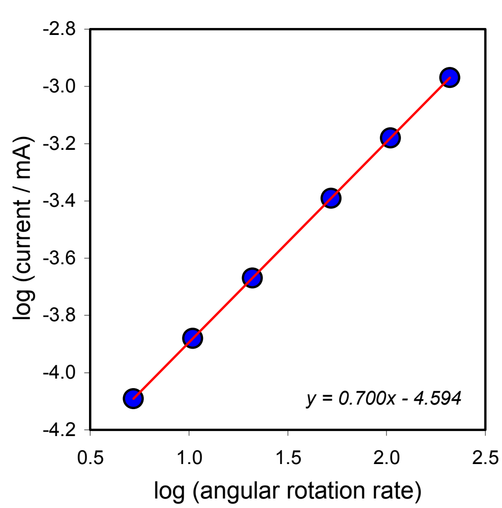

Figure 4: Logarithmic Plot to Test for Mass Transport Limited Corrosion Process

relationship, both the number of electrons exchanged, z, and the bulk concentration, C of the ion or molecule involved in the electrochemical process must be known.

Combining equations (4) and (6), the mass transport limited current density can be expressed as follows:

$$j_{LIM} = 0.0791\, z\, F\, C\, d_{cyl}^{-0.3}\, (\mu/\rho)^{-0.344}\, D^{0.644}\, U_{cyl}^{0.7} \quad (7a)$$

$$= 0.0487\, z\, F\, C\, d_{cyl}^{+0.4}\, (\mu/\rho)^{-0.344}\, D^{0.644}\, \omega^{0.7} \quad (7b)$$

Thus, if a corrosion process is limited by mass transport, it is expected that the limiting current (or limiting current density) will vary linearly with the rotation rate raised to the 0.7 power ($\omega^{0.7}$). Note that this behavior can be verified[28] even without explicit knowledge of z and C simply by conducting a set of measurements at several different rotation rates.

For example, consider a series of LPR scans performed over a range of rotation rates (see Fig. 3). As the rotation rate increases, so does the observed current. A log/log plot of the limiting current (or limiting current density) versus the rotation rate will reveal whether or not the observed current is mass transport limited (see Fig. 4). If the slope of a line drawn through the points on this plot is near 0.7, then this is good evidence that the corrosion process is limited by mass transport.

Modeling Pipeline Flow

A critical issue when attempting to use the RCE to match or mimic a field corrosion condition is choosing the proper rotation rate at which to perform electrochemical measurements. Several solutions to this problem have been proposed[20–35] over the years. Most involve operating the RCE at a rotation rate where the wall shear stress matches that found in the field, or alternately, at a rate where the mass transport coefficient at the RCE matches that observed in the field.

The discussion here will be limited to the latter case, but at the outset, it is important to note that modeling a field corrosion situation in the laboratory involves some compromise and some assumptions. When an RCE is operated at a rotation rate which produces similar mass transport conditions to those found in the field, it is assumed[28] that the corrosion mechanism occurring in the field will be reproduced in the laboratory. However, it is not expected that the actual corrosion rate at the RCE will match that found in the field. There have been specific cases where the RCE failed[20] to reproduce the field corrosion condition. Particular attention is required when surface roughness[7–10,28] influences mass transport. And lastly, there are practical limitations[29] on the range of pipe diameters accessible with the RCE method.

Table II – Rotation Rate Correlation for Water between a Typical* RCE and Smooth, Straight Pipe Flow

Pipe Velocity			Standard Schedule 40 Pipe Sizes (actual ID shown in centimeters)								
(ft/sec)	(cm/sec)	(mile/hour)	2 in 5.25cm	4 in 10.23cm	6 in 15.41cm	8 in 20.27cm	**10 in** 25.45cm	12 in 30.32cm	16 in 38.1cm	18 in 42.88cm	24 in 57.48cm
0.1	3.0	0.07	11	10	9	9	8	8	8	8	7
0.2	6.1	0.14	26	23	22	21	20	19	19	18	17
0.3	9.1	0.20	44	39	36	34	33	32	31	30	29
0.4	12.2	0.27	63	56	52	49	47	46	44	43	41
0.5	15.2	0.34	83	74	68	65	63	61	58	57	54
0.6	18.3	0.41	104	93	86	82	79	76	73	72	68
0.7	21.3	0.48	126	112	104	99	95	92	89	87	82
0.8	24.4	0.55	149	133	123	117	113	109	105	103	97
0.9	27.4	0.61	173	154	143	136	130	126	121	119	113
1.0	30.5	0.68	197	175	163	155	149	144	139	136	129
2.0	61.0	1.36	469	417	387	369	354	343	329	323	306
3.0	91.4	2.05	779	692	643	612	588	570	547	535	508
4.0	122	2.73	1116	991	921	877	842	816	784	767	728
5.0	152	3.41	1475	1310	1217	1159	1113	1079	1036	1014	962

* These quantities assume a typical Pine RCE tip (d_{cyl} = 1.2 cm, A = 3.0 cm^2) being rotated in water at 25ºC. For pure water at 25ºC, the density is 0.997 g cm^{-3} and the absolute viscosity is 0.00891 g cm^{-1} s^{-1}. Computations assume diffusivity, $D = 1.0 \times 10^{-5}$ $cm^2\ s^{-1}$, and a bulk concentration, $C = 1.0 \times 10^{-6}$ mol cm^{-3}.

With these caveats in mind, a computational approach outlined in several reports by Silverman[21–29] (who, in turn, references reports by Wranglen[30], Holser[31], Chen[32] and Nesic[33]) is summarized here. Consider turbulent flow through a smooth, straight pipe. If the flow rate through the pipe, U_p (cm s^{-1}), is known, then the target surface velocity, U_{cyl} (cm s^{-1}), at an RCE which produces a nearly equivalent mass transport condition can be estimated[28] as,

$$U_{cyl} = 0.1185\ (\rho/\ \mu)^{1/4}\ (d_{cyl}^{3/7}\ /\ d_p^{5/28})\ Sc^{-0.0857}\ U_p^{5/4} \quad (8)$$

where d_p (cm) is the diameter of the pipe. Using this relationship together with equation (2), it is possible to compute a target rotation rate for the RCE.

Equation (8) has too many parameters to plot convenient working curves on a graph. To convey some idea of the type of results produced using this equation, Table II lists the velocity/rotation rate relationships for a typical Pine RCE (d_{cyl} = 1.2 cm, A = 3.0 cm^2) operating in pure water. As an example, if water is flowing through a smooth 10-inch Schedule 40 pipe at 1.0 ft/sec, an RCE should be operated at about 149 RPM to match the conditions in the pipe. Note that on-line resources to aid in these kinds of computations are available at the following URL:

http://www.argentumsolutions.com

Reprints

Reprints of this document are available from
Pine Research Instrumentation
5908 Triangle Drive
Raleigh, North Carolina 27617
+1 (919) 782-8320
www.pineinst.com/echem

References

1. M Eisenberg, CW Tobias and CR Wilke, *Ionic Mass Transfer and Concentration Polarization at Rotating Electrodes*, Journal of the Electrochemical Society 101 (1954) 306. http://www.electrochem.org
2. M Eisenberg, CW Tobias and CR Wilke, Chem. Eng. Progr. Symp. Ser. 51 (1955) 1.
3. DR Gabe, *Rotating Cylinder Electrode*, Journal of Applied Electrochemistry 4 (1974) 91. http://dx.doi.org/10.1007/BF00609018
4. DR Gabe and DJ Robinson, *Mass Transfer in a Rotating Cylinder Cell–I. Laminar Flow*, Electrochemica Acta 17 (1972) 1121. http://dx.doi.org/10.1016/0013-4686(72)90028-X
5. DR Gabe and DJ Robinson, *Mass Transfer in a Rotating Cylinder Cell–II. Turbulent Flow*, Electrochemica Acta 17 (1972) 1129. http://dx.doi.org/10.1016/0013-4686(72)90029-1
6. DR Gabe and FC Walsh, *The Rotating Cylinder Electrode: A Review of Development*, Journal of Applied Electrochemistry 13 (1983) 3. http://dx.doi.org/10.1007/BF00615883
7. DR Gabe and FC Walsh, *Enhanced Mass Transfer at the Rotating Cylinder Electrode–I. Characterization of a Smooth Cylinder and Roughness Development in Solutions of Constant Concentration*, Journal of Applied Electrochemistry 14 (1984) 555. http://dx.doi.org/10.1007/BF00626299
8. DR Gabe and FC Walsh, *Enhanced Mass Transfer at the Rotating Cylinder Electrode–II. Development of Roughness for Solutions of Decreasing Concentration*, Journal of Applied Electrochemistry 14 (1984) 565. http://dx.doi.org/10.1007/BF00626300
9. DR Gabe and FC Walsh, *Enhanced Mass Transfer at the Rotating Cylinder Electrode–III. Pilot and Production Plant Experience*, Journal of Applied Electrochemistry 15 (1985) 807. http://dx.doi.org/10.1007/BF00614358
10. DR Gabe and PA Makanjuola, *Enhanced Mass Transfer Using Roughened Rotating Cylinder Electrodes in Turbulent Flow*, Journal of Applied Electrochemistry 17 (1987) 370. http://dx.doi.org/10.1007/BF01023303
11. DR Gabe, GD Wilcox, J Gonzalez-Garcia and FC Walsh, *The Rotating Cylinder Electrode: Its Continued Development and Application*, Journal of Applied Electrochemistry 28 (1998) 759. http://dx.doi.org/10.1023/A:1003464415930
12. G Kear, BD Barker, K Stokes and FC Walsh, *Flow Influenced Electrochemical Corrosion of Nickel Aluminum Bronze – Part I. Cathodic Polarization*, Journal of Applied Electrochemistry 34 (2004) 1235. http://dx.doi.org/10.1007/s10800-004-1758-1
13. G Kear, BD Barker, K Stokes and FC Walsh, *Flow Influenced Electrochemical Corrosion of Nickel Aluminum Bronze – Part II. Anodic Polarization and Derivation of the Mixed Potential*, Journal of Applied Electrochemistry 34 (2004) 1241. http://dx.doi.org/10.1007/s10800-004-1759-0
14. Q Lu, MM Stack and CR Wiseman, *AC Impedance Spectroscopy as a Technique for Investigating Corrosion of Iron in Hot Flowing Bayer Liquors*, Journal of Applied Electrochemistry 31 (2001) 1373. http://dx.doi.org/10.1023/A:1013824010279
15. JM Maciel and SML Agostinho, *Use of a Rotating Cylinder Electrode in Corrosion Studies of a 90/10 Cu–Ni Alloy in* 0.5M H_2SO_4 *Media*, Journal of Applied Electrochemistry 30 (2000) 981. http://dx.doi.org/10.1023/A:1004081212358
16. A Meštrović-Markovinović and DJ Matić, *Mass transfer to a Rotating Horizontal Cylinder Electrode with Full and Partial Immersion*, Journal of Applied Electrochemistry 14 (1984) 675. http://dx.doi.org/10.1007/BF00626312
17. JM Grau and JM Bisang, *Mass Transfer Studies at Rotating Cylinder Electrodes of Expanded Metal*, Journal of Applied Electrochemistry 35 (2005) 285. http://dx.doi.org/10.1007/s10800-004-6770-y

18. A Eklund and D Simonsson, *Enhanced Mass Transfer to a Rotating Cylinder Electrode with Axial Flow*, Journal of Applied Electrochemistry 18 (1988) 710. http://dx.doi.org/10.1007/BF01016897
19. L Labraga, N Bourabaa and T Berkah, *Wall Shear Stress from a Rotating Cylinder in Cross Flow using the Electrochemical Technique*, Experiments in Fluids 33 (2002) 488. http://dx.doi.org/10.1007/s00348-002-0504-x
20. KD Efird, EJ Wright, JA Boros and TG Hailey, *Correlation of Steel Corrosion in Pipe Flow with Jet Impingement and Rotating Cylinder Tests*, Corrosion 49 (1993) 992. http://www.nace.org
21. DC Silverman, *Rotating Cylinder Electrode for Velocity Sensitivity Testing*, Corrosion 40 (1984) 220. http://www.nace.org
22. DC Silverman and ME Zerr, *Application of the Rotating Cylinder Electrode – E-Brite® 26-1 in Concentrated Sulfuric Acid*, Corrosion 42 (1986) 633. http://www.nace.org
23. DC Silverman, *Rotating Cylinder Electrode – Geometry Relationships for Prediction of Velocity-Sensitive Corrosion*, Corrosion 44 (1988) 42. http://www.nace.org
24. DC Silverman, *Corrosion Prediction in Complex Environments using Electrochemical Impedance Spectroscopy*, Electrochimica Acta 38 (1993) 2075. http://dx.doi.org/10.1016/0013-4686(93)80342-W
25. DC Silverman and DJ Kalota, *Behavior of Aspartic Acid as a Corrosion Inhibitor for Steel*, Corrosion 50 (1994) 138. http://www.nace.org
26. DC Silverman, *On Estimating Conditions for Simulating Velocity-Sensitive Corrosion in the Rotating Cylinder Electrode*, Corrosion 55 (1999) 1115. http://www.nace.org
27. DC Silverman, *Technical Note: Simplified Equation for Simulating Velocity-Sensitive Corrosion in the Rotating Cylinder Electrode at Higher Reynolds Numbers*, Corrosion 59 (2003) 207. http://www.nace.org
28. DC Silverman, *The Rotating Cylinder Electrode for Velocity-Sensitive Corrosion – A Review*, Corrosion 60 (2004) 1003. http://www.nace.org
29. DC Silverman, *Technical Note: Conditions for Similarity of Mass-Transfer Coefficients and Fluid Shear Stresses between the Rotating Cylinder Electrode and Pipe*, Corrosion 61 (2005) 515. http://www.nace.org
30. G Wranglen, J Berendson and G Karlberg, *Apparatus for Electrochemical Studies of Corrosion Processes in Flowing Systems*, in Physico-Chemical Hydrodynamics, edited by B Spalding (London: Adv. Publications, 1977) 461.
31. RA Holser, G Prentice, RB Pond and R Guanti, *Use of Rotating Cylinder Electrodes to Simulate Turbulent Flow Conditions in Corrosion Systems*, Corrosion 46 (1990) 764. http://www.nace.org
32. TY Chen, AA Moccari and DD Macdonald, *Development of Controlled Hydrodynamic Techniques for Corrosion Testing*, Corrosion 48 (1992) 239. http://www.nace.org
33. S Nesic, GT Solvi and S Skjerve, *Comparison of Rotating Cylinder and Loop Methods for Testing CO_2 Corrosion Inhibitors*, British Corrosion Journal 32 (1997) 269. http://www.nace.org
34. ASTM G 170, *Standard Guide for Evaluating and Qualifying Oilfield and Refinery Corrosion Inhibitors in the Laboratory* (2001). http://www.astm.org
35. ASTM G 185, *Standard Practice for Evaluating and Qualifying Oil Field and Refinery Corrosion Inhibitors Using the Rotating Cylinder Electrode* (2006). http://www.astm.org

